Korean J. Chem. Eng., 35(6), 1341-1347 (2018)
DOI: 10.1007/s11814-018-0027-7

pISSN: 0256-1115
eISSN: 1975-7220

Gd^{3+} doped Fe_3O_4 nanoparticles with proper magnetic and supercapacitive characteristics: A novel synthesis platform and characterization

Mustafa Aghazadeh*,†, Isa Karimzadeh, Mohammad Ghannadi Maragheh*, and Mohammad Reza Ganjali***,****

*Materials and Nuclear Research School, NSTRI, P. O. Box 14395-834, Tehran, Iran
**Department of Physics, Bonab Branch, Islamic Azad University, Bonab, Iran
***Center of Excellence in Electrochemistry, Faculty of Chemistry, University of Tehran, Tehran, Iran
****Biosensor Research Center, Endocrinology and Metabolism Molecular-Cellular Sciences Institute, Tehran University of Medical Sciences, Tehran, Iran
(*Received 9 May 2017 • accepted 7 February 2018*)

Abstract−A novel electrochemical procedure was developed for the facile preparation of Gd-doped iron oxide nanoparticles (GdIO-NPs). A simple galvanostatic deposition (i=10 mA cm^{-2}) was done in an additive-free aqueous solution containing $FeCl_2{\cdot}4H_2O$, $Fe(NO_3)_3{\cdot}9H_2O$ and $GdCl_3{\cdot}6H_2O$. The XRD, FE-SEM, EDS and TEM characterizations showed that the product is composed of 15% GdIO-NPs with 10 nm in size. VSM analysis proved that the GdIO-NPs are superparamagnetic. The cyclic voltammetry and charge-discharge tests showed that the prepared GdIO-NPs are capable to deliver specific capacity as high as 190.1 F g^{-1} at 0.5 A g^{-1} and capacity retention of 95.1% after 2000 cycling. Based on the results, it was concluded that the developed electrochemical strategy acts as an efficient procedure for the preparation of lanthanide doped MNPs with proper magnetic and supercapacitive characters.

Keywords: Iron Oxide, Gd Ion Doping, Nanoparticles, Electrodeposition, Magnetic Materials, Supercapacitors

INTRODUCTION

As one of the most promising types of energy storage devices, supercapacitors (SCs) are interesting candidates in the fields of backup power systems, portable electronics, telecommunications, vehicles, and so on, for storing the intermittent electrical energy [1]. Electrode materials are the key affecting components on the performance of SCs. According to the energy storage mechanism, SCs electrode materials are usually divided into two types: electric double layer capacitive and pseudocapacitive materials. It was established that on transition metal oxides and hydroxides, including Co_3O_4 [2-5], NiO [6-11], WO_3 [11], MnO_2 [12-19], $Co(OH)_2$ [20-28], $Ni(OH)_2$ [29-33], Fe_2O_3 [34-36] and Fe_3O_4 [37-40] are interesting candidates for use in SCs, and a variety of their nanostructures such as particles, wires, plates or sheets, spheres, rods, nanocapsules and worms have been applied as electro-active materials. Among these materials, iron oxides have attracted much attention due to their variable oxidation states, natural abundance, low cost, as well as environmental friendliness [41]. However, the specific capacitance and high charge/discharge rates of different Fe_3O_4 are significantly limited because of the intrinsically low electrical conductivity, which hinders their widespread application in commercial supercapacitors [42,43]. To overcome these obstacles, several strategies, including mixing composite with carbon-based material (i.e., graphene, carbon nanotubes,...) [44-46], doping with metal ions [47], and designing new nanostructure [48-50] has been proposed. The results of these manipulations on iron oxide electrode indicated that an improvement of supercapacitive performance is observed because of enhancing the conductivity, increasing the surface area, shortenening the diffusion paths and redox activity. Notably, metal ion doping strategy has been rarely investigated.

Lanthanide ions are interesting doping agents due to their optical and magnetic character, which originates from their electronic configurations, and researches have proved that doping magnetic NPs with these ions improves the magnetic properties of iron oxides: saturation magnetization, remanent magnetization, and coercivity [51]. In this regard, Gd-doped iron oxide nanoparticles (GdIO-NPs) have been reported to possess interesting properties [52], where given iron oxide NPs to exhibit better magnetic and plasmonic natures required for potential bio-applications like as bio-sensors, bio-imaging, and therapeutics. Various procedures including chemical precipitation, thermal decomposition, and solvothermal and hydrothermal approaches have been used for the synthesis of GdIO-NPs [51-54]. It has been reported that cathodic electrodeposition acts as a powerful tool for the preparation of pure and/or coated iron oxides [55-60]. To the best of our knowledge, the electrochemical synthesis of GdIO-NPs has not been reported until now. In this work, we used the cathodic deposition technique for preparation of GdIO-NPs with proper magnetic (negligible remanent magnetization and coercivity) and supercapacitive (high specific capacitance and charge-discharge rate) behaviors. The prepared nanoparticles were characterized by XRD, IR, FE-SEM, VSM, cyclic voltammetry (CV) and galvanostat charge-discharge (GCD) techniques. The results of these analyses confirmed the suitable magnetic and super-

†To whom correspondence should be addressed.
E-mail: maghazadeh@aeoi.org.ir, mustafa.aghazadeh@gmail.com

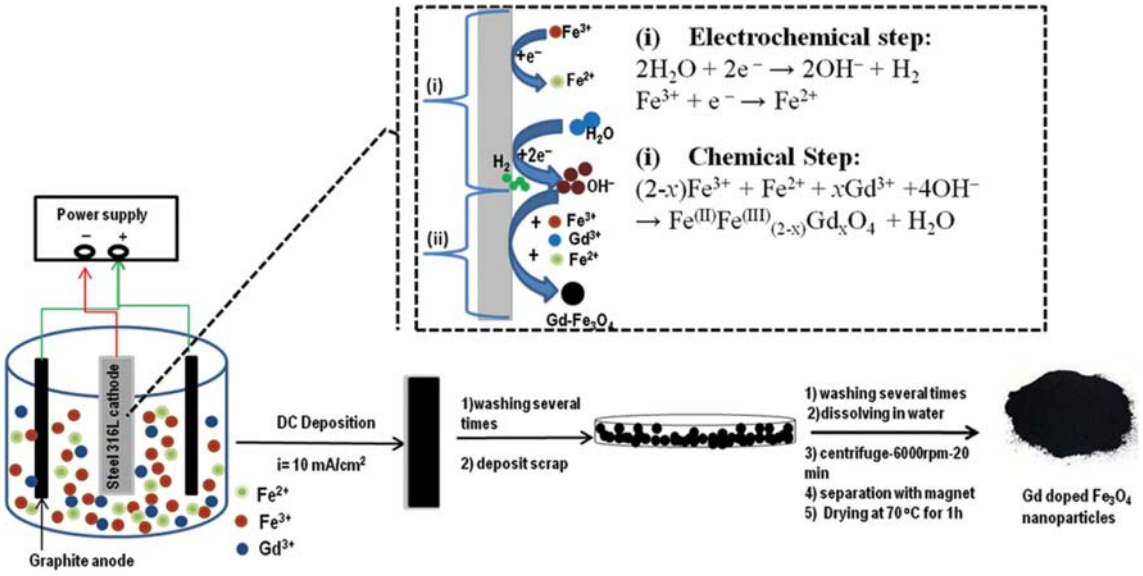

Fig. 1. Schematic route for the electrosynthesis of Gd^{3+} doped Fe_3O_4 nanoparticles; the inset presents the electrochemical (i) and chemical (ii) steps for the formation of Gd-Fe_3O_4 on the surface of the cathode.

capacitive behavior of the prepared Gd-Fe_3O_4 nanoparticles.

EXPERIMENTAL PROCEDURE

1. Materials

Ferrous chloride tetrahydrate ($FeCl_2 \cdot 4H_2O$, 99.5%), ferric nitrate nonahydrate ($Fe(NO_3)_3 \cdot 9H_2O$, 99.9%), gadolinium chloride ($GdCl_3 \cdot 6H_2O$, 99.5%) and polyvinylidene fluoride (PVDF, $(CH_2CF_2)_n$) were purchased from Sigma Aldrich. All materials were used as received without any purification.

2. Electrosynthesis of Gd-doped Magnetite Nanoparticles

An electrochemical synthesis procedure as reported in Refs. [57-59] was used was for the preparation of the products. A schematic view of electrosynthesis procedure and involved reactions is shown in Fig. 1. Based on the general procedure, $FeCl_2 \cdot 4H_2O$ (1.6 g), $Fe(NO_3)_3 \cdot 9H_2O$ (3.4 g) and $GdCl_3 \cdot 6H_2O$ (0.7 g) were dissolved in one liter of deionized water and used as the deposition electrolyte. A two-electrode system including a stainless-steel cathode centered between two graphite anodes was used as the electrodeposition set-up, as shown in Fig. 1. The deposition experiment was conducted by applying a current density of 10 mA cm^{-2}. The deposition time and bath temperature were 30 min and 25 °C, respectively. This process lead to the formation of black deposit on the cathode surface. The formed deposit was then removed from the electrolyte and rinsed several times with distilled water to remove free anions. The deposit was scraped from cathode and dispersed in water, washed repeatedly with water, and separated by magnet. The obtained wet-powder was then dried in a vacuum oven at 70 °C for 1 h, as shown in Fig. 1. The resulting dry black powder was labeled GdIO-NPs.

3. Instruments

The morphology of the prepared powder was observed by field-emission scanning electron microscopy (FE-SEM, Mira 3-XMU with accelerating voltage of 100 kV). The crystal structure of the prepared powder was studied by X-ray diffraction (XRD, Phillips PW-1800) using a Co Kα radiation. The FTIR spectra were obtained using a Bruker Vector 22 Fourier transform infrared spectroscope. Each FTIR spectrum was collected after 20 scans at a resolution of 4 cm^{-1} from 400 to 4,000 cm^{-1}. The magnetic properties of the prepared naked and coated NPs were assessed in the range of −20,000 to 20,000 Oe at room temperature using vibrating sample magnetometer (VSM, model: Meghnatis Daghigh Kavir Co., Iran). Both the magnetic hysteresis and saturation magnetization of the prepared NPs was determined.

4. Electrochemical Characterization

CV and GCD tests were conducted using a potentiostat (AUTOLAB®, Eco Chemie, PGSTAT 30). The three-electrode set-up applied in the CV and GCD tests was composed of a working GdIO-NPs paste electrode, an Ag/AgCl reference electrode, and a counter platinum wire. The GdIO-NPs working electrode (WE) was fabricated through the well-known paste procedure [32-36]. According to this procedure, the prepared black GdIO-NPs powder was physically mixed with acetylene black (>99.9%) and conducting graphite (with ratio of 75 : 10 : 10), and the mixture was homogenized. Then, 5% wt polyvinylidene fluoride (PVDF) dissolved in N-Methyl-2-pyrrolidone (NMP) was added. After partially evaporating the NMP content of the mixture, the resulting paste was pressed at 10 MPa onto a 1 cm^2 Ni foam. The resulting working electrodes were dried for 5 min at about 150 °C in oven. The mass of the loaded GdIO-NPs powder in the fabricated WE was about 2.3 mg. The CVs were recorded in a 1 M Na_2SO_3 solution in the potential widow of −1.0 and +0.1 V vs. Ag/AgCl. The GCD curves were taken at the different current loads. The SCs of the fabricated WE were calculated using following formula:

$$C = \frac{Q}{m \times \Delta V}, \quad Q = I \times \Delta t \tag{1}$$

EIS measurements were performed in a three-electrode system

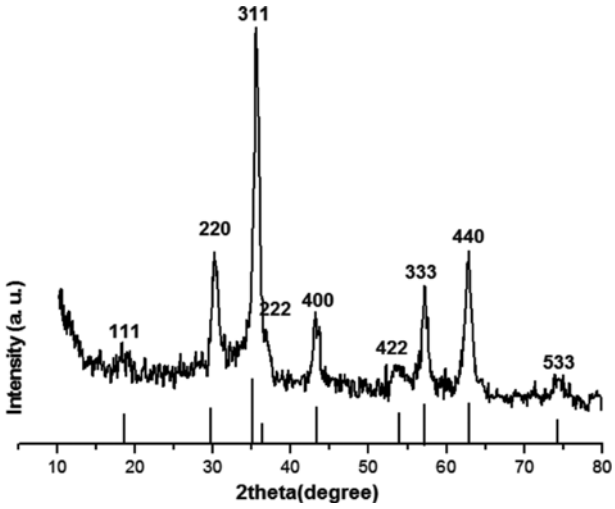

Fig. 2. XRD pattern of the prepared Gd^{3+} doped Fe_3O_4 nanoparticles.

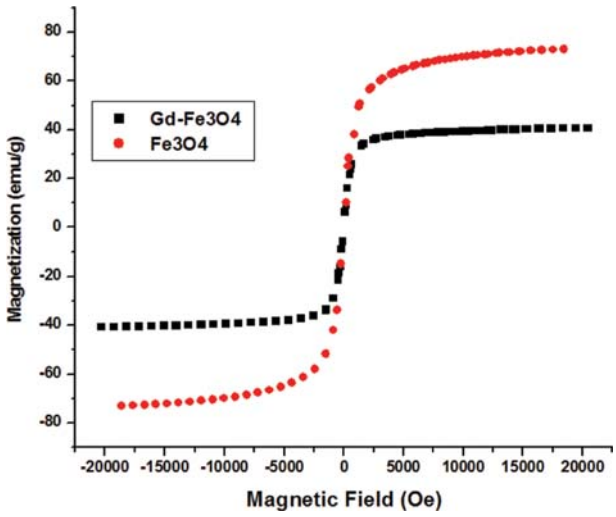

Fig. 4. Hysteresis curves for electrosynthesized the undoped and Gd^{3+} doped Fe_3O_4 nanoparticles.

including GdIO-NPs/or IO-NPs working electrode, Ag/AgCl reference electrode, and a counter platinum wire. The aqueous solution of Na_2SO_3 (1M) was used as the electrolyte. The Nyquist profiles of both prepared working electrodes (i.e., GdIO-NPs and IO-NPs) were recorded under the open circuit potential in an AC frequency range from 10^5 to 10^{-2} Hz with an excitation signal of 5 mV.

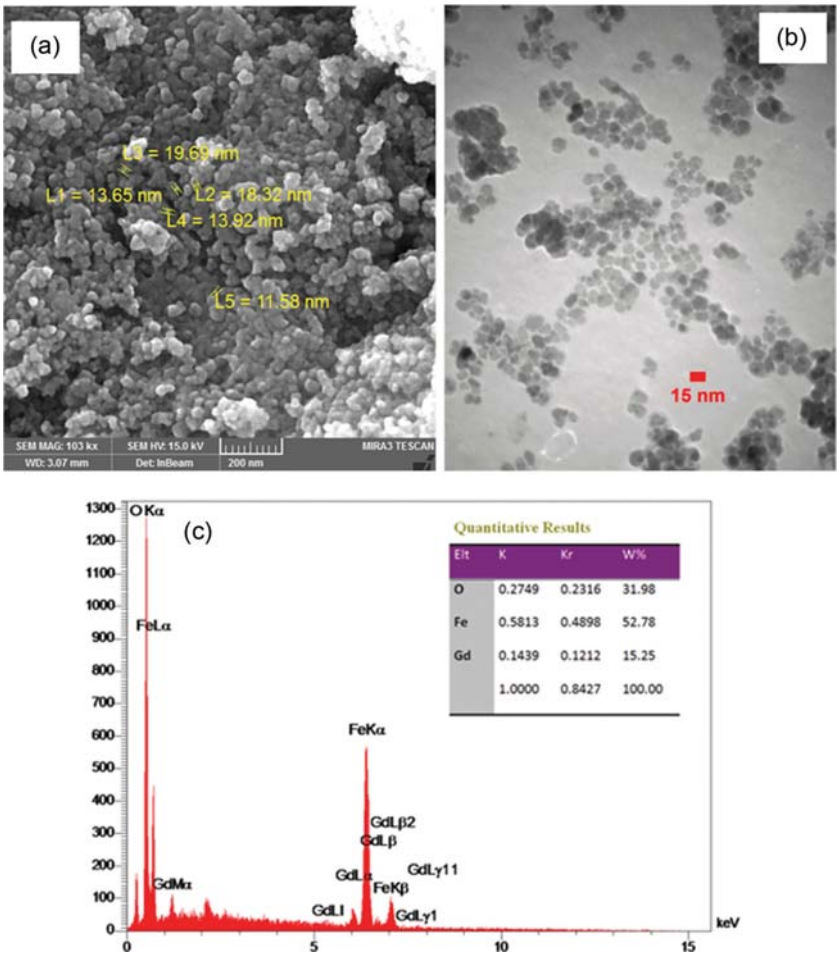

Fig. 3. (a) FE-SEM and (b) TEM images, and (c) EDS analysis of the prepared Gd^{3+} doped Fe_3O_4 nanoparticles.

Table 1. Magnetic data of the prepared Gd^{3+} doped magnetite nanoparticles

Sample name	Ms (emu/g)	Coercivity (Hci) G	Positive (Hci) G	Negative (Hci) G	Negative Mr (emu/g)	Positive Mr (emu/g)	Retentivity Mr (emu/g)
Pure MNPs[a]	72.96	14.6	−41.87	−12.66	0.83	2.73	0.95
GIO-NPs	40.67	6.78	22.53	8.72	−0.41	−1.07	0.33

[a]Data has been provided from Refs. [56,57]

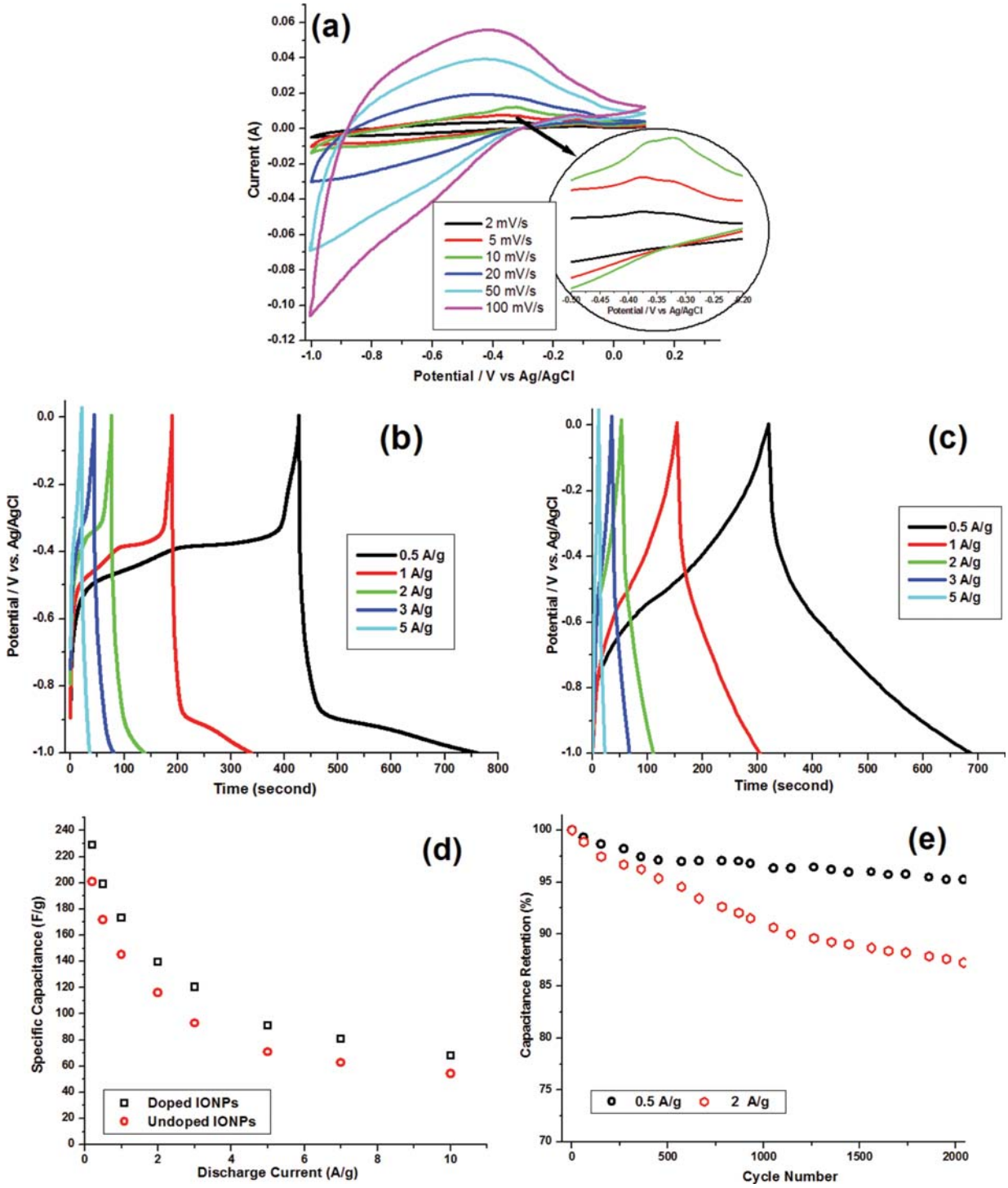

Fig. 5. (a) CVs of GdIO-NPs electrode, (b), (c) GCD curves of the undoped and Gd^{3+} doped electrodes, (d) their SCs at the applied current loads and (e) capacity retentions at 0.5 and 2 A/g. The inset in (a) presents small peaks in the potential range of −0.3 to −0.5 V vs. Ag/AgCl.

RESULTS AND DISCUSSION

1. Structural and Magnetic Analyses

The XRD pattern of the electrosynthesized GdIO-NPs is presented in Fig. 2. In this pattern (Fig. 2), well-defined diffraction peaks of (220), (311), (400), (422), (511), (440), and (533) are clearly observable, which are completely consistent with the characteristic peaks of the Fe_3O_4 phase (JCPDS No. 88-0315). Thus, it can be concluded that no structural changes occurred upon doping of the Fe_3O_4 NPs with Gd, which is in agreement with the results reported in Refs. [51,53].

The average crystallite size (D) of GdIO NPs was calculated to be 9.7 nm using Scherrer's relation ($D=0.9\lambda/\beta\cos(\theta)$).

The FE-SEM image indicates that the sample has a particle-like texture with relative spherical shapes with mean diameter of ~15 nm (Fig. 3(a)). TEM observation in Fig. 3(b) clearly shows the formation of spherical NPs with sizes about 10 nm, which is very close to XRD result: 9.7 nm. The energy-dispersive X-ray (EDX) analysis presented the composition of 52.78% Fe, 15.25% Gd and 31.98% O for the prepared GdIO-NPs (Fig. 3(c)). Based on the fact that some of Fe^{3+} ions have been substituted with Gd^{3+}, these values are very close to Fe_3O_4 composition (27.64% O and 72.36% Fe). Thus, the sample was found to be 15% Gd^{3+} doped Fe_3O_4.

As seen in Fig. 4, the prepared NPs show completely reversible S form than that of un-doped NPs, and no hysteresis can be noticed. The magnetic data for both undoped and Gd doped iron oxide NPs are listed in Table 1. GdIO-NPs exhibited magnetic data of Ms=40.67 emu g^{-1}, Mr=0.33 emu g^{-1} and H_{Ci}=6.87 G. The GdIO-NPs exhibit better superparamagnetic characteristics, i.e., higher Ms and lower Mr and Hc values as compared with those reported in the literature for Sm-MNPs (Ms=31.3 emu g^{-1} and Hc=85.7 G) [51], Eu-MNPs (Ms=23.6 emu g^{-1} and Hc=74.3 G) [52], and as Gd-MNPs (Ms=32.9 and 28.9 emu g^{-1} at 100 and 300 K) [54]. Furthermore, the magnetic data of the prepared GdIO NP were compared with those of the un-doped MNPs reported in Refs. [56,57]: Ms=72.96 emu g^{-1}, Mr=0.95 emu g^{-1} and H_{Ci}=14.61 G. Comparing the data indicated that GdIO-NPs present smaller Mr and H_{Ci} as compared with pure MNPs, which proved their enhanced superparamagnetic nature. Notably, the Ms value is lowered upon Gd doping due to the site preference of Gd ions, the Fe-Gd interactions, as well as the change in the surface effect [53]. Notably, the IONPs with proper magnetic properties are recently interested for use in the various biomedical areas like as cancer diagnosis and therapy, bio-sensing, hyperthermia, cell separation and magnetic resonance imaging (MRI) [61,62]. Hence, these prepared Gd-IONPs could find such applications in bio-medical area, due to suitable magnetic characters.

2. Charge Storage Analyses

Fig. 5(a) shows the CVs of GdIO-NPs within potential window of −1.0 to 0.1 V vs. Ag/AgCl at different scan rates. The form of the CVs indicates the pseudo-capacitive nature of the electroactive material, which is different from the electric double-layer capacitance mechanism. It has formerly been reported that the charge storage of Fe_3O_4 based electrodes in a Na_2SO_3 solution actually takes place through a combination of both EDLC and pseudocapacitance mechanisms. The latter is known to involve the reduction/oxidation of the adsorbed sulfite anions preset on the surface of iron oxide particles [38,39]. As seen in the inset of Fig. 5(a), the CVs exhibit small humps (i.e. redox peaks) at the potential range of –0.3 to 0.4 V vs. Ag/AgCl. These peaks are due to the redox reactions of sulfite anions adsorbed onto GdIO-NPs [39,41]:

$$2SO_3^{2-}+3H_2O+4e^- \leftrightarrow S_2O_3^{2-}+6OH^- \quad (2)$$

$$S_2O_3^{2-}+3H_2O+8e^- \leftrightarrow 2S^-+6OH^- \quad (3)$$

GCD profiles of both undoped and Y^{3+} doped electrodes were also recorded at current densities as shown in Figs. 5(b) and (c). The GCD profiles of the fabricated WEs can be divided into parts; first a symmetric triangular form at V<−0.4 V, and second, non-linear potential dependency at V>−0.4 V. The first part confirms the pure double layer behavior. The second part indicates the typical pseudocapacitance behavior of the IONPs and GdIO-NPs as a result of the faradic reactions. Using Eq. (1), the calculations revealed that the GdIO-NPs are capable of delivering SCs as high as 190.1 F g^{-1} at 0.5 A g^{-1}, 173.3 F g^{-1} at 1 A g^{-1}, 139.5 F g^{-1} at 2 A g^{-1}, 119.4 F g^{-1} at 3 A g^{-1} and 90.7 F g^{-1} at 5 A g^{-1}, respectively (Fig. 5(d)). This data confirmed the excellent super-capacitive behavior for the GdIO-NPs. Fig. 5(d) presents the cyclability of GdIO-NPs during 2000 GCD cycles. Furthermore, the capacitances of the undoped working electrode were also determined from its GCD profiles in Fig. 5(c), which the calculated SC values are presented in Fig. 5(d) and compared with those of Gd cations doped WE. The calculations indicated that the undoped IONPs provides SC values of 171 F g^{-1}, 145 F g^{-1}, 115 F g^{-1}, 92 F g^{-1}, 70 F g^{-1} and 62 F g^{-1} at the discharging loads of 0.5, 1, 2, 3 and 5 A g^{-1}, respectively. From these data, it was confirmed that the capacitance value of the iron oxide nanoparticles in increased up to 15% through gadolinium cations doping into the magnetite structure. The capacity retentions of 95.1% and 87.2% were observed after 2000 cycling at current loads of 0.5 and 2 A g^{-1}, respectively (Fig. 5(e)). These data confirmed that the GdIO-NPs have proper cycle life in Na_2SO_3 electrolyte. The GdIO-NPs were further studied through EIS technique. Fig. 6 presents

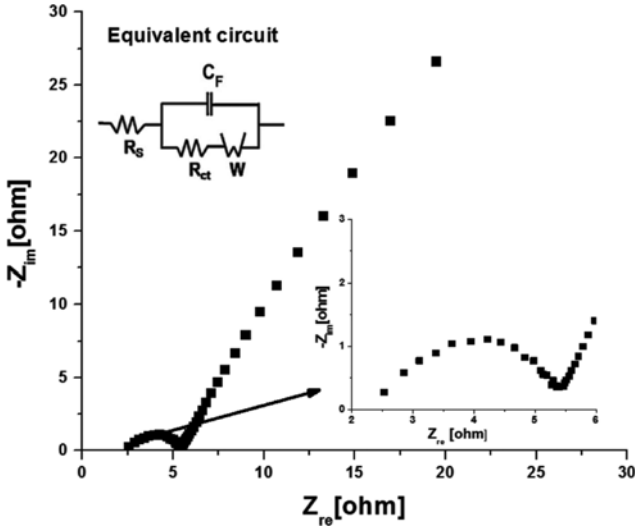

Fig. 6. Nyquist plot for the fabricated electrode with suggested equivalent circuit model.

the Nyquist plot of the GdIO-NPs working electrode in 10 Hz to 100 kHz. This plot can be fitted to an equivalent circuit comprising of an electrolyte resistance (R_s), a double layer capacitor (C_{dl}), a charge transfer resistance (R_{ct}), a Warburg element (Z_w) and a pseudocapacitor (C_p) as shown in the inset of Fig. 6. In fact, there is a semicircle in the frequency range of 100 kHz to 19 kH, and after this range of frequency, the Warburg section is presented in the frequencies of about 19-5 kHz. The straight line section is also observed in the frequency zone of 5 to 0.01 kHz. The R_s and R_{ct} were found to be 2.37 Ω and 2.1 Ω. These low values indicate that the GdIO-NPs working electrode can show excellent supercapacitive performance. Furthermore, the nearly ideal straight line along the imaginary axis at the lower frequencies indicates that the GdIO-NPs working electrode have a low diffusion resistance. The above EIS results proved the excellent charge storage abilities observed form CV and GCD tests.

CONCLUSION

A novel one-pot procedure was introduced for lanthanide ions doping into iron oxide structure. Gd^{3+} doped iron oxide nanoparticles were easily fabricated based on this method. The prepared GdIO-NPs exhibited proper superparamagnetic behavior (Ms=40.67 emu g^{-1}, Mr=0.33 emu g^{-1}) and supercapacitive performance (specific capacitance of 139.5 F g^{-1} and capacity retention of 87.2% at current load of 2 A g^{-1}). Based on the results, our developed electrochemical platform can be used as an effective and easy procedure for the synthesis of Gd^{3+} doped iron oxide nanoparticles.

REFERENCES

1. K. Ulbrich, K. Hola, V. Subr, A. Bakandritsos, J. Tucek and R. Zboril, *Chem. Rev.*, **116**, 5338 (2016).
2. M. Aghazadeh, R. Ahmadi, D. Gharailou, M. R. Ganjali and P. Norouzi, *J. Mater. Sci.: Mater. Electron.*, **27**, 8623 (2016).
3. M. Aghazadeh, *J. Appl. Electrochem.*, **42**, 89 (2012).
4. M. Aghazadeh, M. Hosseinifard, B. Sabour and S. Dalvand, *Appl. Surf. Sci.*, **287**, 187 (2013).
5. N. Venugopal, W. S. Kim and T. Yu, *Korean J. Chem. Eng.*, **33**, 1500 (2016).
6. M. G. Jeong, K. Zhuo, S. Cherevko and C. H. Chung, *Korean J. Chem. Eng.*, **29**, 1802 (2012).
7. M. Aghazadeh and M. R. Ganjali, *Ceram. Int.*, **44**, 520 (2018).
8. M. Aghazadeh, *J. Mater. Sci.: Mater. Electron.*, **28**, 3108 (2017).
9. A. Barani, M. Aghazadeh, M. R. Ganjali, B. Sabour, A. A. M. Barmi and S. Dalvand, *Mater. Sci. Semiconduct. Process.*, **23**, 85 (2014).
10. M. Aghazadeh and M. R. Ganjali, *J. Mater. Sci.: Mater. Electron.*, **28**, 8144 (2017).
11. N. Madhukar Shinde, A. D. Jagadale, V. S. Kumbhar, T. R. Rana, J. H. Kim and C. D. Lokhande, *Korean J. Chem. Eng.*, **32**, 974 (2015).
12. R. Poonguzhali, N. Shanmugam, R. Gobi, A. Senthilkumar, G. Viruthagiri and N. Kannadasan, *J. Power Sources*, **293**, 790 (2015).
13. M. Aghazadeh, A. Bahrami-Samani, D. Gharailou, M. Ghannadi Maragheh and M. R. Ganjali, *J. Mater. Sci.: Mater. Electron.*, **27**, 11192 (2016).
14. M. Aghazadeh, M. R. Ganjali and P. Norouzi, *J. Mater. Sci.: Mater. Electron.*, **27**, 7707 (2016).
15. J. Tizfahm, M. Aghazadeh, M. G. Maragheh, M. R. Ganjali and P. Norouzi, *Mater. Lett.*, **167**, 153 (2016).
16. X. Huang, M. Kim, H. Suh and I. Kim, *Korean J. Chem. Eng.*, **33**, 2228 (2016).
17. M. Aghazadeh, M. Asadi, M. G. Maragheh, M. R. Ganjali and P. Norouzi, *Appl. Surf. Sci.*, **364**, 726 (2016).
18. M. Aghazadeh, M. G. Maragheh, M. R. Ganjali, P. Norouzi and F. Faridbod, *Appl. Surf. Sci.*, **364**, 141 (2016).
19. M. Aghazadeh, M. R. Ganjali and P. Noruzi, *Thin Solid Films*, **634**, 24 (2017).
20. E. M. Jin, H. J. Lee, H. B. Jun and S. M. Jeong, *Korean J. Chem. Eng.*, **34**, 891 (2017).
21. M. Aghazadeh, A. A. Malek Barmi, D. Gharailou, M. H. Peyrovi, B. Sabour and F. Najafi, *Appl. Surf. Sci.*, **283**, 871 (2013).
22. G. H. Jeong, H. M. Lee, H. Lee, C. K. Kim, Y. Piao, J. H. Lee, J. H. Kim and S. W. Kim, *RSC Adv.*, **4**, 51619 (2014).
23. M. Aghazadeh and S. Dalvand, *J. Electrochem. Soc.*, **161**, D18 (2014).
24. M. Aghazadeh, S. Dalvand and M. Hosseinifard, *Ceram. Int.*, **40**, 3485 (2014).
25. M. Aghazadeh, H. Mohammad Shiri and A. A. Malek Barmi, *Appl. Surf. Sci.*, **273**, 237 (2013).
26. M. Aghazadeh and M. R. Ganjali, *J. Mater. Sci.: Mater. Electron.*, **28**, 11406 (2017).
27. J. Talat Mehrabad, M. Aghazadeh, M. Ghannadi Maragheh and M. R. Ganjali, *Mater. Lett.*, **184**, 223 (2016).
28. M. Aghazadeh, A. Rashidi and M. R. Ganjali, *Electronic. Mater. Lett.*, **14**, 37 (2018).
29. J. Gou, S. Xie, Y. Liu and C. Liu, *Electrochim. Acta*, **210**, 915 (2016).
30. J. Tizfahm, B. Safibonab, M. Aghazadeh, A. Majdabadi, B. Sabour and S. Dalvand, *Colloids Surf. A*, **443**, 544 (2014).
31. M. Aghazadeh, M. Ghaemi, A. N. Golikand and A. Ahmadi, *Mater. Lett.*, **65**, 2545 (2011).
32. M. Aghazadeh, M. Ghaemi, B. Sabour and S. Dalvand, *J. Solid State Electrochem.*, **18**, 1569 (2014).
33. M. Aghazadeh, B. Sabour, M. R. Ganjali and S. Dalvand, *Appl. Surf. Sci.*, **313**, 581 (2014).
34. A. A. Yadav, *J. Mater. Sci.: Mater. Electron.*, **27**, 12876 (2016).
35. M. Aghazadeh, I. Karimzadeh and M. R. Ganjali, *J. Mater. Sci.: Mater. Electron.*, **28**, 18121 (2017).
36. M. Zhang, J. Sha, X. Miao, E. Liu, C. Shi, J. Li, C. He, Q. Li and N. Zhao, *J. Alloys Compd.*, **696**, 956 (2017).
37. E. Mitchell, R. K. Gupt, K. Mensah-Darkw, D. Kumar, K. Ramasamy, B. K. Gupta and P. Kahol, *New J. Chem.*, **38**, 4344 (2014).
38. V. D. Nithya and N. Sabari Arul, *J. Power Source*, **327**, 297 (2016).
39. L. Wang, H. Ji, S. Wang, L. Kong, X. Jiang and G. Yang, *Nanoscale*, **5**, 3793 (2013).
40. M. Aghazadeh, I. Karimzadeh and M. R. Ganjali, *Mater. Lett.*, **209**, 450 (2017).
41. V. D. Nithya and N. Sabari Arul, *J. Mater. Chem. A.*, **4**, 10767 (2016).
42. Z. Zhou, W. Xie, S. Li, X. Jiang, D. He, S. Peng and F. Ma, *J. Solid State Electrochem.*, **19**, 1211 (2015).
43. Y. Yang, J. Li, D. Chen and J. Zhao, *ACS Appl. Mater. Interfaces*, **8**, 26730 (2016).
44. S. Chen, R. Zhou, Y. Chen, Y. Fu, P. Li, Y. Song and L. Wang, *J.*

Nanopart. Res., **19**, 127 (2017).
45. Y. Z. Wu, M. Chen, X. H. Yan, J. Ren, Y. Dai, J. J. Wang, J. M. Pan, Y. P. Wang and X. N. Cheng, *Mater. Lett.*, **198**, 114 (2017).
46. H. Fan, R. Niu, J. Duan, W. Liu and W. Shen, *ACS Appl. Mater. Interfaces*, **8**, 19475 (2016).
47. X. Yang, J. Kan, F. Zhang, M. Zhu and Z. Li, *J. Inorg. Org. Polym. Mater.*, **27**, 542 (2017).
48. X. Tang, R. Jia, T. Zhai and H. Xia, *ACS Appl. Mater. Interfaces*, **7**, 27518 (2015).
49. T. Xia, X. Xu, J. Wang, C. Xu, F. Meng, Z. Shi, J. Lian and J. M. Bassat, *Electrochim. Acta*, **160**, 114 (2015).
50. W. M. Zhang, X. L. Wu, J. S. Hu, Y. G. Guo and L. J. Wan, *Adv. Funct. Mater.*, **18**, 3941 (2008).
51. C. R. De Silva, S. Smith, I. Shim, J. Pyun, T. Gutu, J. Jiao and Z. Zheng, *J. Am. Chem. Soc.*, **131**, 6336 (2009).
52. J. C. Park, S. Yeo, M. Kim, G. T. Lee and J. H. Seo, *Mater. Lett.*, **181**, 272 (2016).
53. H. Zhang, V. Malik, S. Mallapragada and M. Akinc, *J. Magn. Magn. Mater.*, **423**, 386 (2017).
54. F. J. Douglas, D. A. MacLaren, N. Maclean, I. Andreu, F. J. Kettles and F. Tuna, *RSC Adv.*, **6**, 74500 (2016).
55. I. Karimzadeh, M. Aghazadeh, M. R. Ganjali, P. Norouzi, T. Doroudi and P. H. Kolivand, *Mater. Lett.*, **189**, 290 (2017).
56. I. Karimzadeh, M. Aghazadeh, M. R. Ganjali, P. Norouzi, S. Shirvani-Arani, T. Doroudi, P. H. Kolivand, S. A. Marashi and D. Gharailoud, *Mater. Lett.*, **179**, 5 (2016).
57. M. Aghazadeh and M. R. Ganjali, *J. Mater. Sci.: Mater. Electron.*, **29**, 4981 (2018).
58. I. Karimzadeh, M. Aghazadeh, M. R. Ganjali and T. Dourudi, *Curr. Nanosci.*, **13**, 167 (2017).
59. I. Karimzadeh, H. Rezagholipour Dizaji and M. Aghazadeh, *Mater. Res. Express*, **3**, 095022 (2016).
60. M. Aghazadeh and M. R. Ganjali, *J. Mater. Sci.*, **53**, 295 (2018).
61. Z. Bakhtiary, A. A. Saei, M. J. Hajipour, M. Raoufi, O. Vermesh and M. Mahmoudi, *Nanomed.*, **12**, 287 (2016).
62. K. Ulbrich, K. Hola, V. Subr, A. Bakandritsos, J. Tucek and R. Zboril, *Chem. Rev.*, **116**, 5338 (2016).